

Complete Fusion of Weakly Bound Nuclei Applying the Delayed X-Ray Technique: the ${}^9\text{Be} + {}^{144}\text{Sm}$ System

P. R. S. Gomes¹, I. Padron^{1,*}, O. A. Capurro², J. O. Fernández Niello², G. V. Martí², R. M. Anjos¹, J. Lubian¹, R. Veiga¹, E. Crema³, A. J. Pacheco², J. E. Testoni², A. Arazi², M. D. Rodríguez^{2,4}, M. E. Ortega^{2,4}, and M. Trotta⁵

¹Instituto de Física, Universidade Federal Fluminense, Niterói, R.J., 24210-340, Brazil

²Laboratorio Tandem, Departamento de Física, Comisión Nacional de Energía Atómica, Av. del Libertador 8250, (1429), Buenos Aires, Argentina

³Departamento de Física Nuclear, Universidade de São Paulo, Caixa Postal 66318, 05315-970, São Paulo, S.P., Brazil

⁴Departamento de Física, FCEyN, UBA, Buenos Aires, Argentina and

⁵INFN Sezione di Napoli, I-80126, Napoli, Italy. *Permanent address: CEADEN, P.O. Box 6122, Havana, Cuba

Received on 17 December, 2004

The detection of delayed X-rays produced by the decay that follows electron capture in the residual nuclei has been used in the past for the determination of fusion cross sections of tightly bound nuclei. In this work we applied this technique to study the effect of the break-up of a weakly bound projectile, like in the case of the ${}^9\text{Be} + {}^{144}\text{Sm}$ system. Preliminary results of the complete fusion in this system at near barrier energies are presented.

In recent years, the study of the fusion of weakly bound nuclei and the influence of the break-up process on the complete fusion cross section is a subject of great interest in nuclear physics, particularly due to the availability of radioactive beams with very low bound energy thresholds. This research can also be done with stable weakly bound nuclei, like ${}^6\text{Li}$, ${}^7\text{Li}$ and ${}^9\text{Be}$, which have break-up threshold energies from 1.45 MeV to 2.65 MeV, much lower than the usual 8 – 10 MeV required to break-up a tightly bound nucleus.

The study of complete-fusion (CF) reactions using weakly bound projectiles generally presents great difficulties. This occurs because the corresponding evaporation residues are very similar to, or even coincident with, those coming from incomplete fusion (ICF), i.e., reactions in which one of the break-up fragments of the projectile fuses with the target. Therefore, what is usually measured is the total fusion cross section, that is, the sum of CF and ICF cross sections instead of the individual contributions required to investigate the effect of the break-up process on the CF cross section.

Separate measurements of CF and ICF cross sections for the ${}^9\text{Be}$, ${}^{6,7}\text{Li} + {}^{208}\text{Pb}$, ${}^{209}\text{Bi}$ systems were performed at Canberra and Legnaro [1–4] using the detection of decay alpha particles. The residual nuclei of the fusion of these systems decay by alpha emission with life times compatible with typical irradiation and detection times. These experiments found that for these heavy targets, the ICF is responsible for suppression of the order of 25 – 30% of the CF cross section, at energies above the Coulomb barrier.

There are some experimental evidence [5, 6] that this CF suppression becomes negligible when light mass targets are used. One needs to perform experiments with different and lighter targets, if one wants to fully understand the process. However, the fusion residues of lighter systems do not decay by the emission of alpha particles.

As an alternative method, we propose the off-line detection of the X-rays produced when the residual nuclei decay by electron capture with half-lives from some minutes to several hours. This method was successfully applied by our

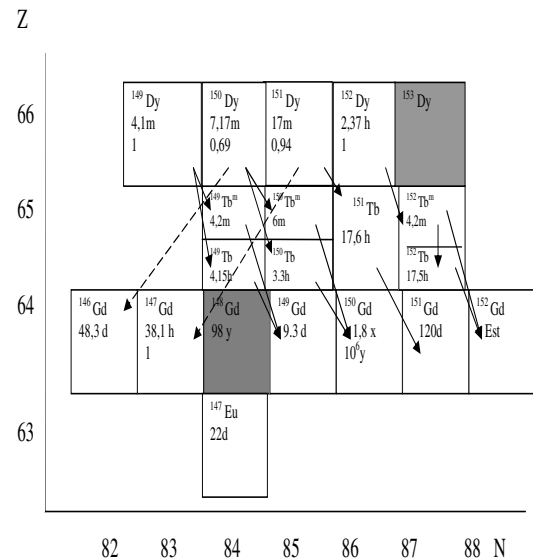


FIG. 1: Decay characteristics of the complete fusion compound nucleus ${}^{153}\text{Dy}$ and the incomplete fusion compound nucleus ${}^{148}\text{Gd}$.

groups [7–11] for the study of sub-barrier fusion of tightly bound nuclei.

We have searched for systems with ${}^{6,7}\text{Li}$ and ${}^9\text{Be}$ as projectiles and targets not too heavy that produce CF residual nuclei decaying by electron capture (EC) different from those present in the case of ICF. The primary selected target was ${}^{144}\text{Sm}$.

The next step was to verify quantitatively the predictions of the evaporation code PACE [12] for the evaporation of the compound nucleus for each of these systems. The most suitable system was found to be ${}^9\text{Be} + {}^{144}\text{Sm}$, as it will be explained in the following.

Figure 1 shows the region of the nuclide chart that illustrates the decay of the evaporation residues of the compound nuclei produced by CF (i.e. ${}^9\text{Be} + {}^{144}\text{Sm}$) and ICF (i.e. $\alpha +$

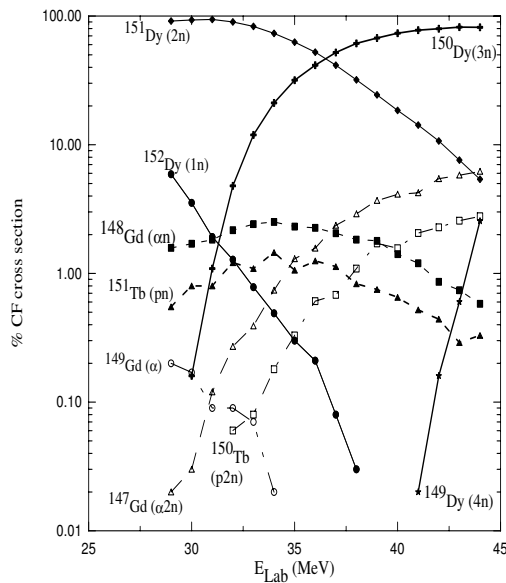


FIG. 2: Predictions of the evaporation code PACE for the evaporation following the complete fusion of ${}^9\text{Be} + {}^{144}\text{Sm}$.

${}^{144}\text{Sm}$), ${}^{153}\text{Dy}$ and ${}^{148}\text{Gd}$, respectively.

Figure 2 shows the predictions of the code PACE for the CF of the ${}^9\text{Be} + {}^{144}\text{Sm}$ system, corresponding to the energy range from $0.8 V_B$ to $1.4 V_B$, where V_B is the height of the Coulomb barrier.

The predictions of the code PACE for the ICF of $\alpha + {}^{144}\text{Sm}$, assuming that the energy of the α particle is $[4/9 E({}^9\text{Be}) - S_n]$, where $S_n = 1.57$ MeV is the break-up threshold energy for the fragmentation of ${}^9\text{Be}$ in $n + 2\alpha$, can be obtained. The code predicts that the two main evaporation channels produce the ${}^{148}\text{Gd}$ and ${}^{147}\text{Gd}$ nuclei at this energy range (near to the Coulomb barrier for the $\alpha + {}^{144}\text{Sm}$ system). The first is almost stable, whereas the second can be measured, although at high energies it may be slightly contaminated by one CF evaporation channel.

The experiment was performed at the Tandem Laboratory in Buenos Aires. A target of BeO was used to produce ${}^9\text{Be}$ beams, with energies from $E_{\text{Lab}} = 29$ MeV to 44 MeV, with a 1 MeV interval, ranging from sub-barrier to above barrier energies. Five 88% enriched ${}^{144}\text{Sm}$ targets were used, with thicknesses from $170 \mu\text{g}/\text{cm}^2$ to $230 \mu\text{g}/\text{cm}^2$ and carbon backings of $20 \mu\text{g}/\text{cm}^2$.

An aluminum catcher foil was placed a few millimeters behind the target. The suitable catcher foil thickness of $1.6 \text{ mg}/\text{cm}^2$ was chosen in such way that it should stop the fusion residues and leave the elastic scattering particles go through. During the irradiation of the target, the beam intensity was recorded by multi-scaling in one-minute intervals. One surface barrier silicon detector - placed at 30 degrees with the beam direction - was used as monitor for normalization purposes. The typical irradiation time was 2 hours.

Due to the fact that a fraction of the fusion residues with the lowest energies were trapped in the target, after each irra-

diation we removed the target and the catcher foil and placed both of them in front of the a LEP (Low Energy Photon) detector. Since each target was used more than one time, the residual X-ray counting rate from the previous irradiation was accumulated, in order to subtract the background. Typically, five minutes passed between the end of an irradiation and the beginning of the X-ray accumulation spectra.

For the detection of the delayed K X-rays, a LEP germanium detector was used. The lines to be analyzed were the $K_{\alpha 1}$ and $K_{\alpha 2}$ X-rays from Tb, Gd and Eu, with energies in the range from 40.90 to 44.48 keV. The energy separation of the peaks was around 700 eV, and since energy resolution of the detector was $\Delta E_{FWHM} = 600$ eV at the energy range of the K_{α} X-rays, it was possible to resolve the lines. Furthermore, since the relations between the $K_{\alpha 1}$ and $K_{\alpha 2}$ X-rays of each element are well known, they were used to check the consistency of the peak fit procedure. The peak shape was well determined by the Gd X-rays emitted by the standard ${}^{152}\text{Eu}$ calibration source.

As we needed to discriminate between identical X-rays corresponding to isotopes with different half-lives, an automatic set of counting runs was programmed. Due to the half-lives characteristics, the following set of counting periods for the delayed X-rays was used: 3 runs of 5 minutes, 3 runs of 15 minutes and 2 runs of 30 minutes each, corresponding to the total counting time of two hours. For some energies we have also accumulated long runs lasting several hours, in order to improve the statistics of the Eu X-rays corresponding to the $T_{1/2} = 38.1$ hours decay of ${}^{147}\text{Gd}$.

The energy calibration and LEP Ge (HP) detector efficiency were measured using the gamma-ray lines in the range of 30-300 keV of the following standard radioactive sources: ${}^{152}\text{Eu}$, ${}^{133}\text{Ba}$, ${}^{137}\text{Cs}$, ${}^{241}\text{Am}$ and ${}^{57}\text{Co}$.

Figures 3a and 3b show typical KX-ray spectra. Both correspond to the bombarding energy of 40 MeV. The spectrum displayed in figure 3a was obtained from a short run taken a few minutes after the end of the irradiation, whereas the one shown in figure 3b was obtained from a long run taken 90 minutes after the end of the irradiation. One can observe that the relative intensity of the Tb X rays associated with the first decay generation decreases with time, whereas the opposite happens for the Gd X-rays.

For the fusion cross section derivation, we used a code specially written for this purpose, the XRWEPC[13], adapted from the original X-RAY code[14]. The main features of the code can be summarized as follows.

The fusion cross section is written as

$$\sigma_{\text{fusion}} = \sum_A P_A, \quad (1)$$

where P_A are the individual evaporation cross sections while the peak area of the K_{α} X-rays can be expressed as

$$N_{Z-1}(t_I, t_F) = C \sum_A W_{Z,A} F_{Z,A}(t_I, t_F) P_A, \quad (2)$$

being t_I and t_F the initial and final counting time of the run, C is a normalization constant that depends on the Rutherford

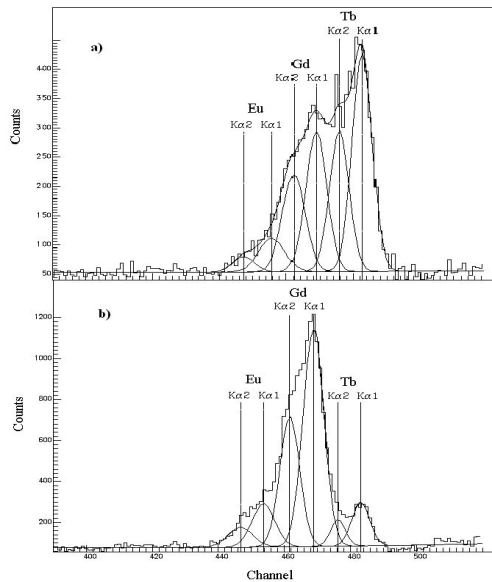


FIG. 3: Typical K_{α} X-ray energy spectra, at laboratory bombarding energy of 40 MeV. The spectrum on the upper part of the figure was obtained from a short run taken a few minutes after the end of the irradiation, whereas the spectrum on the lower part was obtained from a longer run taken 90 minutes after the end of the irradiation.

scattering and the X-ray detector efficiency, $W_{Z,A}$ is the number of K_{α} X-rays produced for each nucleus (Z,A) decay, $F_{Z,A}(t_I, t_F)$ is the number of decays of the nucleus (Z,A) per unitary production of the residues of mass A , which is a function of the time depending on the beam intensity in the irradiation time interval (t_I, t_F) and on the half-lives of the residual nuclei. The coefficients $W(Z,A)$ were taken from [15].

The P_A values are obtained from simultaneous fits of all points of the yields of K_{α} X-rays as a function of time. This procedure allows to check the self consistency, because within one chain corresponding to one value of A there is more than one decay generation.

Figure 4 shows a typical simultaneous fit of the three different X-ray counting rates, as a function of time. One can observe how the time dependence of the X-rays emitted by each element can be decomposed into the corresponding decay of each isotope, with different half-lives.

The fusion data analysis is under way and the cross section values and the interpretation of these reaction mechanisms will be reported in the near future. Within the aims of this paper, we show in figure 5 some preliminary results for the fusion cross section, at some energies, corresponding to the accumulation of X-rays emitted just from the aluminum catcher foil itself and from the set catcher foil + target.

In summary, this work presents an alternative method for the measurement of complete fusion of weakly bound nuclei based on the delayed X-rays technique. This method allows us to distinguish between complete and incomplete fusion if an appropriate system is chosen; that is, systems in which each evaporation residue is fed by only one of the fusion processes. This is the case of the ${}^9\text{Be} + {}^{144}\text{Sm}$ leading to the compound

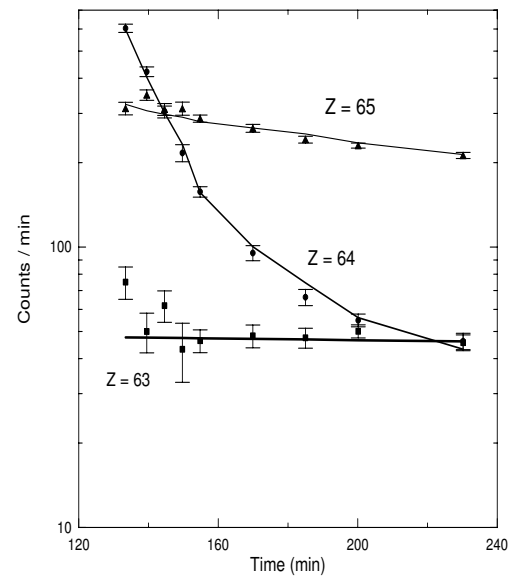


FIG. 4: Typical simultaneous fit of K_{α} X-rays emitted by three different elements, and several isotopes.

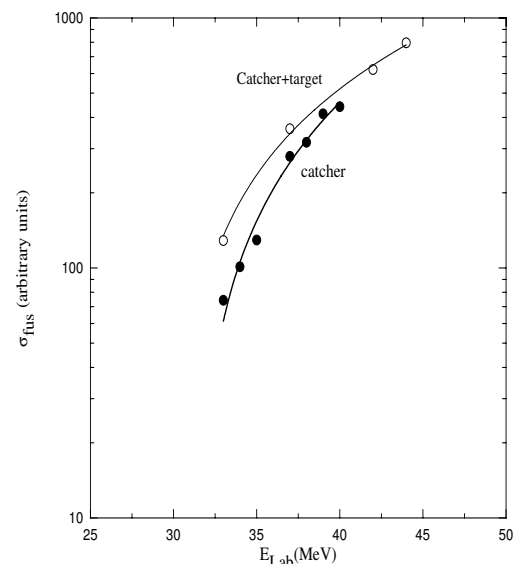


FIG. 5: Preliminary results of the fusion cross section, showing the importance of the measurement of X-rays emitted by both catcher foil and target. When only the catcher foil was placed in front of the detector, only a fraction of the cross section was derived.

nucleus ${}^{153}\text{Dy}$, for which the evaporation residues are different from the residues of the incomplete fusion.

Acknowledgments

The Brazilian authors would like to thank the CNPq, CAPES, FAPERJ and FAPESP for their financial support. JOFN, AJP, and JET acknowledge the financial support of the CONICET.

-
- [1] C. Signorini *et al.*, *Eur. Phys. J. A* **2**, 227 (1998).
[2] M. Dasgupta *et al.*, *Phys. Rev. Lett.* **82**, 1395 (1999).
[3] M. Dasgupta *et al.*, *Phys. Rev. C* **66**, 041602R (2002).
[4] M. Dasgupta *et al.*, *Phys. Rev. C* **70**, 024606 (2004).
[5] S.B. Moraes *et al.*, *Phys. Rev. C* **61**, 64608 (2000).
[6] P.R.S. Gomes *et al.*, *Heavy Ion Physics* **11**, 361 (2000).
[7] D. di Gregorio *et al.*, *Phys. Lett. B* **176**, 322 (1986).
[8] D. di Gregorio *et al.*, *Phys. Rev. C* **39**, 516 (1989).
[9] S. Gil *et al.*, *Phys. Rev. Lett.* **65**, 3100 (1990).
[10] P.R.S. Gomes *et al.*, *Phys. Rev. C* **49**, 245 (1994).
[11] M. di Tada *et al.*, *Phys. Rev. C* **47**, 2970 (1993).
[12] A. Gavron, *Phys. Rev. C* **21**, 230 (1980).
[13] O.A. Capurro, Private communication.
[14] A.J. Pacheco *et al.*, *Comp. Phys. Communications* **52**, 93 (1988).
[15] U. Reus, W. Westmeir, *Atomic Data and Nucl. Data Tables* **29**, n 2 (1983).